RED CELLS, IRON, AND ERYTHROPOIESIS

Congenital dyserythropoietic anemia type III (CDA III) is caused by a mutation in kinesin family member, *KIF23*

Maria Liljeholm,[1] Andrew F. Irvine,[2] Ann-Louise Vikberg,[3] Anna Norberg,[3] Stacy Month,[4] Herbert Sandström,[5] Anders Wahlin,[1] Masanori Mishima,[2] and Irina Golovleva[3]

[1]Department of Radiation Sciences, Umeå University, Umeå, Sweden; [2]Mechanochemical Cell Biology, Division of Biomedical Cell Biology, Warwick Medical School, University of Warwick, Coventry, United Kingdom; [3]Department of Medical Biosciences/Medical and Clinical Genetics, Umeå University, Umeå, Sweden; [4]Department of Pediatric Hematology-Oncology, Kaiser-Permanente, Oakland, CA; and [5]Department of Public Health and Clinical Medicine, Family Medicine, Umeå University, Umeå, Sweden

Key Points

- *KIF23*/MKLP1 mutation found in the CDA III patients causes cytokinesis failure.

Haplotype analysis and targeted next-generation resequencing allowed us to identify a mutation in the *KIF23* gene and to show its association with an autosomal dominant form of congenital dyserythropoietic anemia type III (CDA III). The region at 15q23 where CDA III was mapped in a large Swedish family was targeted by array-based sequence capture in a female diagnosed with CDA III and her healthy sister. Prioritization of all detected sequence changes revealed 10 variants unique for the CDA III patient. Among those variants, a novel mutation c.2747C>G (p.P916R) was found in *KIF23*, which encodes mitotic kinesin-like protein 1 (MKLP1). This variant segregates with CDA III in the Swedish and American families but was not found in 356 control individuals. RNA expression of the 2 known splice isoforms of *KIF23* as well as a novel one lacking the exons 17 and 18 was detected in a broad range of human tissues. RNA interference–based knock-down and rescue experiments demonstrated that the p.P916R mutation causes cytokinesis failure in HeLa cells, consistent with appearance of large multinucleated erythroblasts in CDA III patients. We conclude that CDA III is caused by a mutation in *KIF23*/MKLP1, a conserved mitotic kinesin crucial for cytokinesis. (*Blood*. 2013;121(23):4791-4799)

Introduction

Congenital dyserythropoietic anemia (CDA) is a group of rare hereditary disorders with ineffective erythropoiesis and distinct dyserythropoietic changes in the bone marrow. Three major types (I, II, and III) and several subtypes have been described.[1-3] CDA III is the rarest form of the 3 classical CDAs, with about 60 cases described globally, the majority belonging to a family in Sweden. The disease is characterized by intravascular hemolysis in combination with dyserythropoiesis with large multinucleated erythroblasts (gigantoblasts) in the bone marrow. The anemia is mild to moderate and red blood cell transfusions are rarely needed. In the Swedish family, retinal angioid streaks, monoclonal gammopathy of undetermined significance, and myeloma have also developed in a substantial number of patients.[4] The first family with CDA III identified and described by Wolff and von Hofe in 1951 was an American family consisting of a mother and her 3 affected children. The anemia was named "familial erythroid multinuclearity."[5] Later, a family, with church records dating back to the 18th century was described in the Swedish County Västerbotten and the condition was named benign hereditary erythroreticulosis.[6] A dominant pattern of inheritance was noted in both the American and the Swedish families. A small Argentinean family with autosomal dominant CDA III has also been described.[7]

The few reported sporadic cases of CDA III have shown considerable differences in clinical presentation, with severe erythroid hyperplasia associated with skeletal disorders, mental retardation, and hepatosplenomegaly. The pattern of inheritance seems to be autosomal recessive in these cases, suggesting a different genetic alteration.[8,9]

CDA III, as it appears in the Västerbotten family, has the characteristic morphology in bone marrow smears with large multinucleated erythroblasts. When a bone marrow smear is not available, elevated thymidine kinase or laboratory data indicating intravascular hemolysis, with elevated lactate dehydrogenase (LDH) and undetectable haptoglobin, confirm the CDA III diagnosis, provided that 1 of the parents is affected.[4,10] By linkage analysis the genetic location of CDA III (MIM 105600) was mapped to an 11-cM interval on chromosome 15q21-q25, but the disease gene was not identified.[11]

The genes responsible for recessive forms of CDA, CDA I (MIM 224120), and CDA II (MIM 224100) have been reported. CDA I is caused by mutations in codanin I (*CDAN1*; MIM 607465), also located on chromosome 15, whereas CDA II depends on mutations in a component of coat protein complex II–coated vesicles (*SEC23B*, MIM 610512) situated on chromosome 20.[12-14] Recently, a fourth type of CDA with an autosomal-dominant inheritance pattern (CDA IV, MIM 613673) and genetic defect in a transcriptional activator on chromosome 19p13 (*KLF*, 600599) was identified.[15] In the present study, we aimed at identification of the gene responsible for CDA III.

Submitted October 12, 2012; accepted March 29, 2013. Prepublished online as *Blood* First Edition paper, April 9, 2013; DOI 10.1182/blood-2012-10-461392.

The online version of this article contains a data supplement.

There is an Inside *Blood* commentary in this issue.

The publication costs of this article were defrayed in part by page charge payment. Therefore, and solely to indicate this fact, this article is hereby marked "advertisement" in accordance with 18 USC section 1734.

Materials and methods

Patients and DNA samples

DNA was available from 39 affected and 21 unaffected members of the Swedish family (see supplemental Materials and supplemental Figure 1 on the *Blood* website), and 4 affected and 2 unaffected members of the American family. Clinical and laboratory information for each member of the Swedish family is provided in Table 1. Ethical approval was obtained from the Regional Ethics Committee in Umeå, Sweden, and informed consent was obtained from all patients. The study followed the tenants of the Declaration of Helsinki.

Targeted sequencing and data analysis

DNA samples from 2 sisters, 1 affected and 1 unaffected, from the Swedish family (supplemental Materials, supplemental Figure 1) were selected for targeted sequencing of the candidate region at 15q23 at Ambry Genetics (Aliso Viejo, CA) (http://www.ambrygen.com). Library preparation and indexing were performed using Roche NimbleGen 385k sequence capture array target enrichment, and 54-bp paired-end processing was done using the Illumina GAIIx (San Diego, CA). Initial data processing and base calling, including extraction of cluster intensities, was done using RTA1.8 (SCS version 2.8). Sequence quality filtering script was executed in the Illumina CASAVA software (version 1.7.0). The reads were mapped against University of California San Cruz hg19.

For bidirectional sequencing of *KIF23* (MIM 605064, ENSG00000137807), intronic sequences adjacent to exon 21 were amplified from genomic DNA. Sequences for *KIF23* primers designed with Primer3 software were 21F: 5′gctcattttggaggaacagaa; and 21R: 5′ gggagttcctgatgaagtgg. Polymerase chain reaction (PCR) amplification and the sequencing reactions were performed as described elsewhere.[16] The products of sequencing reactions were analyzed on ABI 3500xL Dx Genetic Analyzer (Applied Biosystems, Foster City, CA). Sequences were aligned and evaluated using Sequencher software version 4.9 (Gene Codes Corporation, Ann Arbor, MI). All identified variants were denoted using accepted nomenclature recommended by the Human Genome Variation Society. To predict the impact of sequence variants on protein function, missense mutations were analyzed by Sorting Intolerant from Tolerant (http://sift.jcvi.org) and Polymorphism Phenotyping (http://genetics.bwh.harvard.edu/pph). Variants detected in intronic sequences were analyzed with the splice site prediction programs GeneSplicer (http://www.cbcb.umd.edu/software/GeneSplicer) and Splice Site Finder (www.genet.sickkids.on.ca/ali/splicesitefinder). All bioinformatics tools were available via the Alamut software version 2.0 (Interactive Biosoftware, Rouen, France).

Sequences of *MYO9A* and *TLE3* specific primers are listed in supplemental Table 1.

KIF23 expression

Reverse transcription (RT)-PCR was performed on First Choice Human Total RNA Survey Panel (Ambion Life Technologies, Carlsbad, CA). We used RNA isolated from the following tissues: brain, colon, heart, kidney, liver, lung, small intestine, spleen, thymus, placenta, ovary, skeletal muscles, prostate, testis, and thyroid. Furthermore, RNA was extracted from the lymphocytes of whole blood of a CDA III patient and a control case. Two sets of *KIF23*-specific primers were used along with *GAPDH* primers. Primer sequences and RT-PCR protocol are given in supplemental Table 2. RT-PCR products were then separated on agarose gel and visualized under ultraviolet light after staining with ethidium bromide.

KIF23 functional analysis

Knock-down and rescue analyses in HeLa cells synchronized by double-thymidine block were performed as previously reported,[17,18] using small interfering RNA (siRNA) targeted to the 3′-untranslated region of *KIF23* and a rescue complementary DNA construct of the KIF23 Δ18 splice isoform (ENST00000559279) tagged with a green fluorescent protein (GFP) at the N terminus. P916R mutation was introduced by site-directed mutagenesis with primers 5′-cttccacagtagcacGtgcccaaccagatgg-3′ and 5′-ccatctggttgggcaCgtgctactgtggaag-3′ and confirmed by sequencing. Time-lapse observation by differential interference contrast and GFP fluorescence microscopy was performed with a DeltaVision system (Applied Precision) equipped with a UPlanFL N 40×/1.30 objective lens (Olympus) and a CoolSNAP HQ2 cooled CCD camera (Photometrics) using softWoRx software (Applied Precision). During imaging, cells were maintained in Dulbecco's modified Eagle medium supplemented with 10% fetal bovine serum, 100 U/mL penicillin, and 100 μg/mL streptomycin in a microscope stage incubator (Tokai Hit) at 37°C and 5% carbon dioxide. Data on cytokinesis failure were analyzed with generalized linear model for binomial data using R (http://www.r-project.org/).

Results

Clinical findings

The diagnosis of CDA III was confirmed in 26 bone marrow smears and excluded in 13 cases (Table 1, Figure 1). When bone marrow smears were not available, thymidine kinase and laboratory data revealing hemolysis were used (Table 1). In the group, without available bone marrow samples, the diagnosis of CDA III was based on elevated thymidine kinase, LDH, and/or undetectable haptoglobin in 11 cases. In 1 case, the diagnosis was based on elevated LDH and haptoglobin alone. CDA III was excluded by normal thymidine kinase and normal LDH and haptoglobin in 6 cases.

Genetic findings

Haplotype and candidate gene analyses. CDA III disease was mapped to 15q21-q25 in 11-cM interval.[11] Analysis of some genes (eg, *CENP8*, *HEXA*, *ARIH1*) in the linkage region by direct sequencing or by denaturing high performance liquid chromatography did not reveal any pathogenic mutations. To find the minimal shared haplotype, genotyping with microsatellite markers was performed 3 times between 1993 and 2004 (supplemental Materials, supplemental Figure 2). Because CDA III patients of younger generation were diagnosed during these years, we expected to find a new recombination event that would allow refining of the disease locus. As a result of haplotype reevaluation, the disease-causative gene was expected to reside in an interval of 2.41 Mb between markers D15S100 and D15S1050 (69571161-71981252) based on a current version of genome sequence (hg 19, BUILD 37.2).

Gene identification. To identify the disease gene within the refined disease locus, DNA from 2 females of the Swedish CDA III family, 1 affected (V: 12) (supplemental Materials, supplemental Figure 1) and her unaffected (V: 13) sister (supplemental Materials, supplemental Figure 1) were selected for targeted sequencing of the candidate region. For this purpose, we decided to cover the region of 3.54 Mb between markers D15S100 and D15S980 (69571161-73113373) (supplemental Materials, supplemental Figure 2).

In total, 29 sequence variants in 13 genes were detected in the affected CDA III individual compared with 23 sequence variants in 12 genes in the healthy sister (supplemental Materials, supplemental Table 3). Ten sequence variants absent in the control sample (V: 13) and unique for the CDA III patient (V: 12) are summarized in Table 2. Because of autosomal dominant inheritance in the CDA III family, 6 homozygous sequence variants in *THAP10, LRRC49*, *GRAMD2*, *HEXA*, and *ADPGK* were excluded from further analysis. Furthermore, all these variants reported previously would not affect protein function according to the bioinformatics tools (Table 2). Two

Table 1. Diagnostic characteristics in the CDA III Swedish family

	Sex	Bone marrow morphology*	Hb, g/L†	Haptoglobin, g/L‡	LDH, μkat/L	Thymidine kinase§	CDA III‖
III:6	M	+	143	<0.1	5.2	52.5	+
III:9	M	−	ND	ND	ND	1.5	−
III:10	M	+	107	<0.1	5.8	36.5	+
III:12	F	−	ND	ND	ND	1.4	−
III:14	M	+	116	0.1	4.3	18.1	+
III:18	M	−	162	0.6	2.7	2.6	−
III:20	F	+	128	<0.1	6.3	36.2	+
IV:2	F	+	80	<0.1	5.3	27.9	+
IV:4	F	+	126	<0.1	8.5	250.0	+
IV:5	M	−	149	1.6	3.1	1.9	−
IV:7	F	+	105	<0.1	8.0	39.1	+
IV:8	M	+	157	<0.1	6.8	37.7	+
IV:10	M	+	107	<0.1	6.2	46.5	+
IV:12IV:12	M	+	ND	ND	ND	56.8	+
IV:14	M	−	153	1.8	2.0	2.2	−
IV:15	M	+	146	<0.1	6.2	28.9	+
IV:17	M	+	129	<0.1	6.2	59.1	+
IV:20	F	+	120	<0.1	4.8	53.3	+
IV:21	F	−	135	1.1	1.9	2.7	−
IV:22	M	−	154	0.6	2	4.5	−
IV:24	F	ND	105	<0.1	ND	65.0	+
IV:26	F	+	114	<0,1	6.1	62.3	+
V:1	M	+	118	<0.1	5.7	43.6	+
V:3	M	+	127	<0.1	7.1	75.0	+
V:4	M	−	145	0.5	2.8	ND	−
V:5	M	+	106	<0.1	6.8	64.3	+
V:7	F	+	94	<0.1	7.7	149.0	+
V:8	F	−	107	0.5	2.4	1.7	−
V:9	M	+	135	<0.1	6.3	65,6	+
V:12	F	ND	114	<0.1	6.7	184.0	+
V:13	F	−	145	1.9	2.0	2.6	−
V:14	M	+	113	<0.1	5.7	41.9	+
V:17	M	−	130	0.6	2.9	1.0	−
V:18	F	−	136	1.0	2.0	3.4	−
V:19	F	ND	153	0.7	2.1	4.0	−
V:20	M	ND	158	1.0	ND	3.3	−
V:22	F	+	121	<0.1	6.1	89.0	+
V:23	M	+	135	<0.1	6.4	139.0	+
V:24	M	ND	105	<0.1	ND	52.3	+
V:26	M	ND	120	<0.1	ND	108.0	+
V:27	M	ND	147	0.6	2.7	5.0	−
V:28	M	ND	145	0.3	3.1	8.0	−
V:30	F	ND	109	<0.1	4.1	120.0	+
V:31	M	ND	118	0.8	ND	3.8	−
V:32	M	ND	127	ND	3.4	7.0	−
V:33	F	+	119	0.1	4.3	18.5	+
V:35	M	ND	ND	<0.1	ND	69.0	+
V:36	F	+	124	<0.1	8.3	167.0	+
V:38	F	−	138	2,6	2.7	6.4	−
VI:1	F	ND	102	<0.1	7.5	279.0	+
VI:2	F	ND	133	1.22	2.2	30.0	−
VI:3	F	ND	114	1.87	2.6	ND	−
VI:4	M	+	123	<0.1	10.0	ND	+
VI:5	M	ND	149	0.53	3.3	ND	−
VI:6	F	ND	116	<0.1	5.9	116	+
VI:7	F	ND	109	<0.1	6.6	120	+
VI:8	M	ND	125	ND	4.6	134	+
VI:10	M	+	108	<0.1	5.8	286	+
VI:11	F	ND	115	ND	5.3	102	+
VI:14	F	ND	107	<0.1	8.8	ND	+

F, female; CDA III Hb, hemoglobin; LDH, lactate dehydrogenase; M, male; ND, no data.

*Consistent with CDA III.

†Normal range for males is 134-170 and for females 117-153.

‡Normal range 0.24-1.9.

§Normal range <3.4, adjusted according to Nordic Reference Interval Project.

‖CDA III final diagnosis.

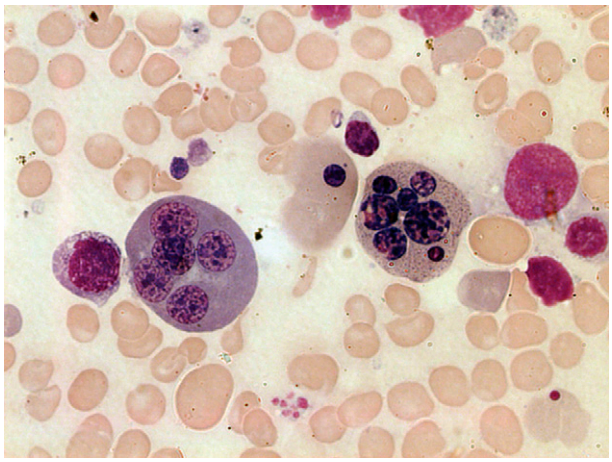

Figure 1. Bone marrow smear from a patient with CDA III. May-Grünwald-Giemsa staining was used and the image was taken by bright field microscopy with 100× objective (Leica DM3000, Leica Microsystems CMS GmbH, Wetzlar, Germany). Two polychromatic erythroblasts, 1 with 7 nuclei (right) and 1 with 5 nuclei (left) are shown. Anisocytic and hypochromatic erythrocytes are also evident.

sequence variants in the *TLE3* gene could also be excluded because c.615G>C resulted in a synonymous amino acid (p.205S>S) and IVS207+3T>C was a common variant present in 23% of the general population (Table 2); however, they were considered for further testing in segregation analysis. Sequence changes in 2 genes, *KIF23* and *MYO9A*, were predicted to be not tolerated and deleterious for protein function. The variant in *MYO9A*, c.4892T>A (p.N1631I) (rs80283650), was previously reported as a rare variant. The most promising gene associated with CDA III was *KIF23*. Novel sequence variant c.2747C>G in exon 21 was confirmed by Sanger sequencing (Figure 2) and resulted in amino acid substitution p.P916R (Table 2).

Segregation analysis. The 2 *TLE3* variants c.615G>C (p.205S>S) and IVS207+3T>C as well as the *MYO9A* variant c.4892T>A (p.N1631I) were excluded as a potential cause of CDA III because they did not segregate with the disease in the Swedish family (data not shown). Furthermore, the c.4892T>A variant in the *MYO9A* gene was detected at a higher frequency in the Swedish population (0.065) compared with the 1000 Genome project (0.011; Table 2).

Segregation analysis of the *KIF23* c.2747C>G variant was done by restriction fragment length polymorphism analysis using the *Hpy*CH4IV endonuclease for digestion of *KIF23* exon 21 in 2 CDA III families of Swedish (data not shown) and American origin (Figure 3). The c.2747C>G (p.P916R) mutation was present in heterozygous form only in affected CDA III patients. Furthermore, the mutation was absent in 356 control individuals from a geographically matched Swedish population. The p.P916R mutation has not been described in the literature previously and is thus novel to both the Swedish and the American families. These data imply that the *KIF23* is a strong candidate gene for causing the disease.

KIF23 expression. *KIF23* encodes mitotic-kinesin-like protein 1 (MKLP1), a highly conserved factor crucial for formation of the central spindle and midbody and thus in the completion of cytokinesis. RNA expression of *KIF23* in 15 different tissues and whole blood of a CDA III patient was analyzed by RT-PCR. Specific primers were designed for detection of the 2 known isoforms generated by alternative splicing of exon 18,[19] ENST00000260363, a full-length (FL) transcript containing exon 18 and encoding a 960AA protein, and ENST00000559279, which lacks exon 18 (Δ18) and encoding a protein of 856AA. Primers specific for exons 16 and 19 detected 2 bands (391 bp and 211 bp) that correspond to the Δ18 transcript and a novel transcript lacking both exons 17 and 18 (Δ17+18), respectively (Figure 4A-B). The identity of these transcripts was confirmed by direct sequencing of the PCR products (supplemental Materials, supplemental Figure 3). However, under our conditions, these primers failed to detect a 703-bp band that corresponds to the FL transcript, although the presence of this transcript was confirmed with the primers specific for the exons 17 and 18. Although expression of the FL and Δ17+18 transcripts was tissue-dependent, the Δ18 transcript was detected in all the tissues examined, including the in peripheral blood of the CDA III patient. Our results were in agreement with the data available via http://biogps.org in which broad *KIF23* expression with the highest level in erythroid precursors is observed.

Functional analysis. To evaluate the effect of the *KIF23* p.P916R mutation on the function of its product, MKLP1, in cytokinesis, a knock-down and rescue assay with the most ubiquitously expressed MKLP1 Δ18 isoform was performed in HeLa cells (Figure 5). In this assay, endogenous MKLP1 was depleted with an siRNA against its 3′ untranslated region (Figure 5A) and RNA interference–resistant MKLP1 constructs tagged with GFP-MKLP1 (Figure 5B) were expressed during synchronization of the cell cycle (supplemental Figure 4). Cytokinesis was monitored by time-lapse imaging. During normal cell division in HeLa cells, anaphase onset triggers formation of the central spindle microtubule bundle between segregating chromosomes (Figure 5D, yellow arrows), with MKLP1 highly accumulating to the central antiparallel overlap zone (white arrow). This induces cleavage furrow ingression at the cell equator. Compacted by the ingressing furrow, the central spindle matures into the midbody (arrowhead), which maintains the intercellular bridge up to several hours until the daughter cells are finally separated by

Table 2. Sequence variants in CDA III patient detected by targeted resequencing

Gene	Nucleotide change	Mutation form	Amino acid change	dbSNP	SIFT	PolyPhen	MAF
KIF23	c.2747C>G	Heterozygous	p.916P>R	New variant	Not tolerated	Deleterious	
MYO9A	c.4892T>A	Heterozygous	p.1631N>I	rs80283650	Not tolerated	Possibly damaging	A = 0.011/24
TLE3	c.615G>C	Heterozygous	p.205S>S	rs17759219	Not predictable	Not predictable	NA
TLE3	IVS297+3T>CT	Heterozygous		rs2291986	Not predictable	Not predictable	C = 0.228/497
THAP10	c.117A>G	Homozygous	p.39G>G	rs2955035	Not predictable	Not predictable	A = 0.486/1061
LRRC49	c.1061_1063delAAC	Homozygous	p.Q354del	rs56720495	Not predictable	Not predictable	NA
GRAMD2	IVS134+23A>C	Homozygous		rs11072348	Not predictable	Not predictable	A = 0.05/109
HEXA	c.1306T>C	Homozygous	p.436I>V	rs1800431	Tolerated	Benign	T = 0.101/220
ADPGK	c.551T>C	Homozygous	p.184K>R	rs8024644	Tolerated	Possibly damaging	C = 0.195/426
ADPGK	c.546A>G	Homozygous	p.182G>G	rs8023358	Not predictable	Not predictable	G = 0.184/402

dbSNP, Single Nucleotide Polymorphism Database; MAF, minor allele frequency (established in 1000 Genome project); NA, not available; PolyPhen, Polymorphism Phenotyping; SIFT, Sorting Intolerant from Tolerant.

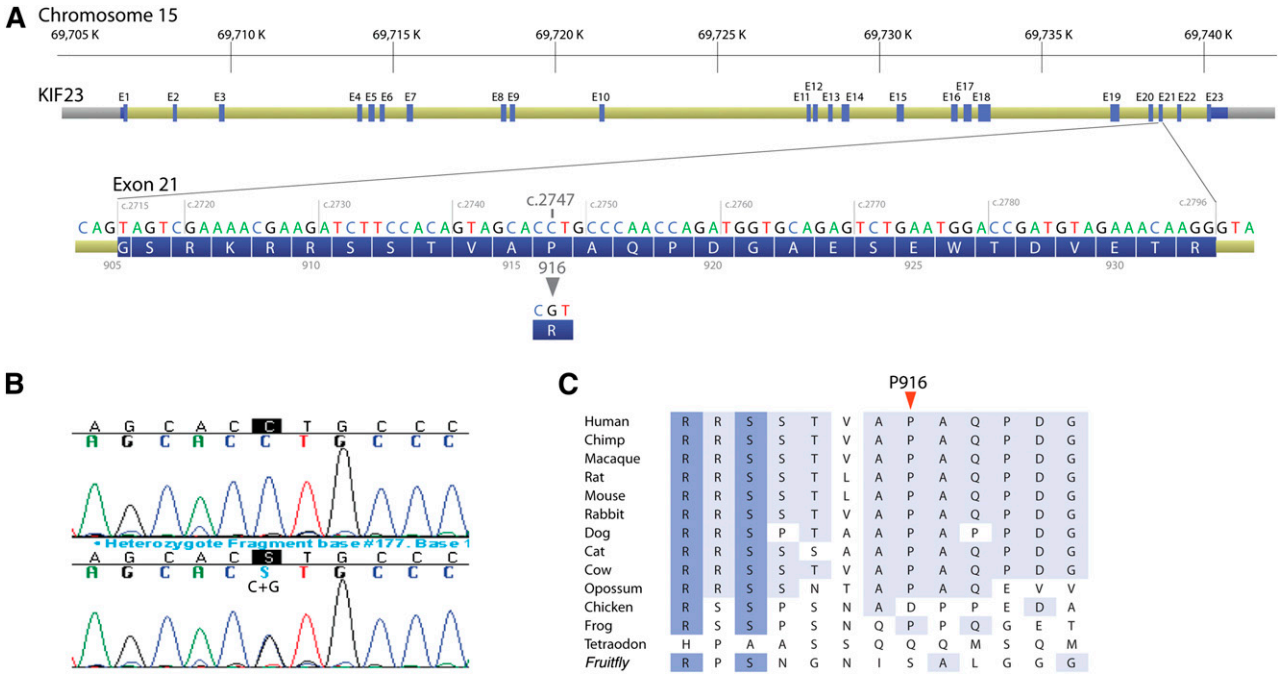

Figure 2. A novel c.2747C>G (p.P916R) mutation in the *KIF23* gene. (A) Exon structure of the *KIF23* gene with DNA and protein sequence of the exon 21 where the mutation resides. (B) DNA sequence showing c.2747C>G mutation. (Upper) Wild type and (lower) c.2747C>G heterozygous mutations, with mutation position marked in black. (C) Phylogenetic alignment of partial *KIF23* protein sequence.

abscission (double-headed arrow). MKLP1 plays essential roles in the formation of the central spindle and the stable maintenance of the midbody. Failure of cytokinesis by depletion of the endogenous MKLP1 was efficiently rescued by expression of wild-type GFP-MKLP1 (Figure 5C). In contrast, GFP-MKLP1 with the p.P916R mutation (P812R mutation in this isoform) showed little or no rescue activity above the level of the control empty vector (Figure 5C, P916R vs GFP). Cells expressing GFP-MKLP1-P916R could complete constriction of the cleavage furrow and form the midbody in a similar time course with the cells expressing the wild-type GFP-MKLP1, but regressed to form binucleate cells about 2 hours after midbody formation (180 ± 148 nub [mean ± standard deviation.], mode at 105 min, n = 225) (Figure 5D-E and supplemental Videos 1 and 2). These data indicate that the p.P916R mutation impairs the function of MKLP1 essential for the completion of cytokinesis.

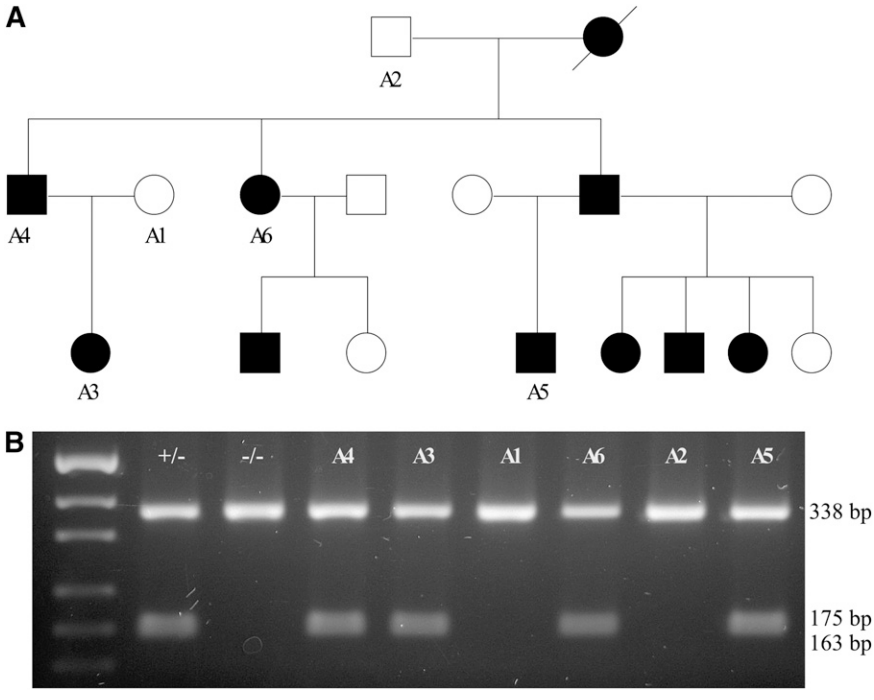

Figure 3. c.2747C>G segregates CDA III in the American family. (A) Pedigree of the family with affected individuals shown in black symbols and healthy individuals shown as unfilled symbols. DNA was available only for cases marked with A1–A6. (B) Restriction length fragment polymorphism assay. Amplification of exon 21 of *KIF23* was done as described in "Materials and Methods." PCR products were digested using the *Hpy*CH4IV endonuclease. c.2747C>G creates a restriction site; therefore, all mutation carriers show 3 bands—338, 175, and 163 bp (small fragments are poorly resolved on agarose gel)—whereas all unaffected individuals show only 1 band (338 bp).

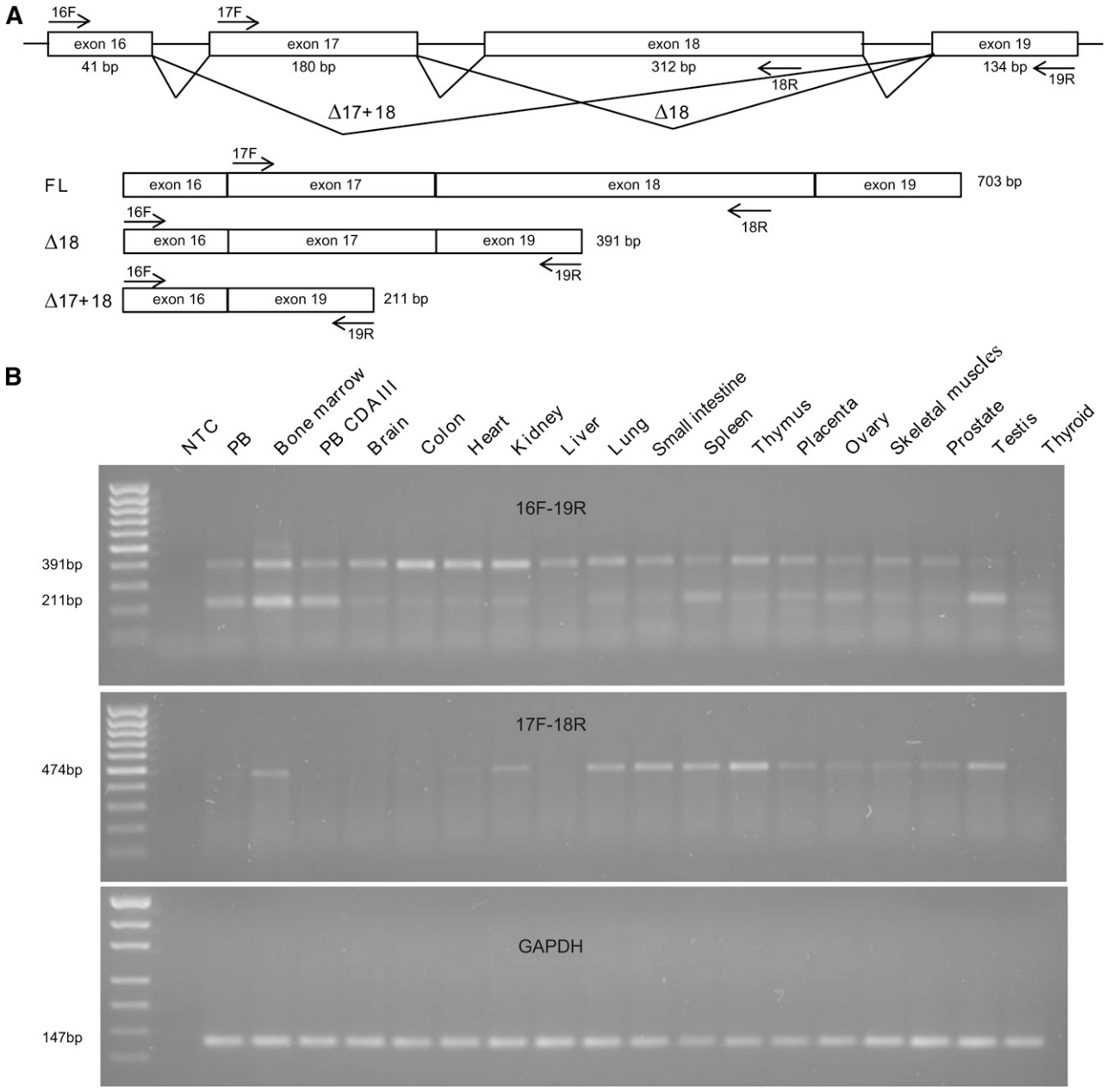

Figure 4. RNA expression of *KIF23*. (A) Schematic representation of alternative splicing of the exons 17 and 18 of *KIF23*. The primers used for RT-PCR are indicated by arrows. Two previously reported transcripts (FL and Δ18) as well as a novel one (Δ17+18) are illustrated with the expected sizes of the RT-PCR products. (B) Detection of *KIF23* transcripts and a control glyceraldehyde-3-phosphate dehydrogenase (GAPDH) transcript in a broad range of tissues by RT-PCR with primers 16F and 19R (top), 17F and 18R (middle), and GAPDH primers (bottom). Under these conditions, the primers 16F and 19R detected the Δ18 and Δ17+18 transcripts but not the FL transcript, although its expression was observed with the primers 17F and 18R (FL). MassRuler Low Range DNA Ladder (80-1031 bp) and pUC19DNA/*MspI* (*HpaII*) Marker, 23 (Thermo Fisher Scientific, Inc., Waltham, MA) were used as a size standard for *KIF23* and *GAPDH*, respectively.

Discussion

The genetic cause of the rarest form of CDA, CDA type III, was identified in this study almost 2 decades after its chromosomal localization was detected. At the time of DNA and laboratory sampling, 10 of the CDA III–positive individuals and 6 of the CDA III–negative individuals were younger than age 18, explaining why bone marrow investigation was not done in all cases. Moreover, it was difficult to motivate all individuals in the family to undergo a bone marrow aspiration because the diagnosis in this family can be determined by laboratory sampling of peripheral blood. A previously shown correlation of CDA III with elevated LDH and undetectable haptoglobin in this family was confirmed in this study. Analysis of these parameters in 25 of the 26 CDA III–positive individuals, diagnosed by bone marrow morphology, showed elevated LDH and undetectable haptoglobin in all cases. Twelve CDA III negative individuals, without signs of the disease in the bone marrow, showed normal levels of haptoglobin and LDH. Thymidine kinase analyzed in 25 out of 26 morphology-based CDA III–positive cases spanned from 18.1 to 289 U/L. This is far higher than the normal range in adults, which is set to less than 5 U/L. However, in 1 16-year-old female in the CDA III–negative group diagnosed by bone marrow examination, the thymidine kinase was 6.4 U/L. As discussed in an

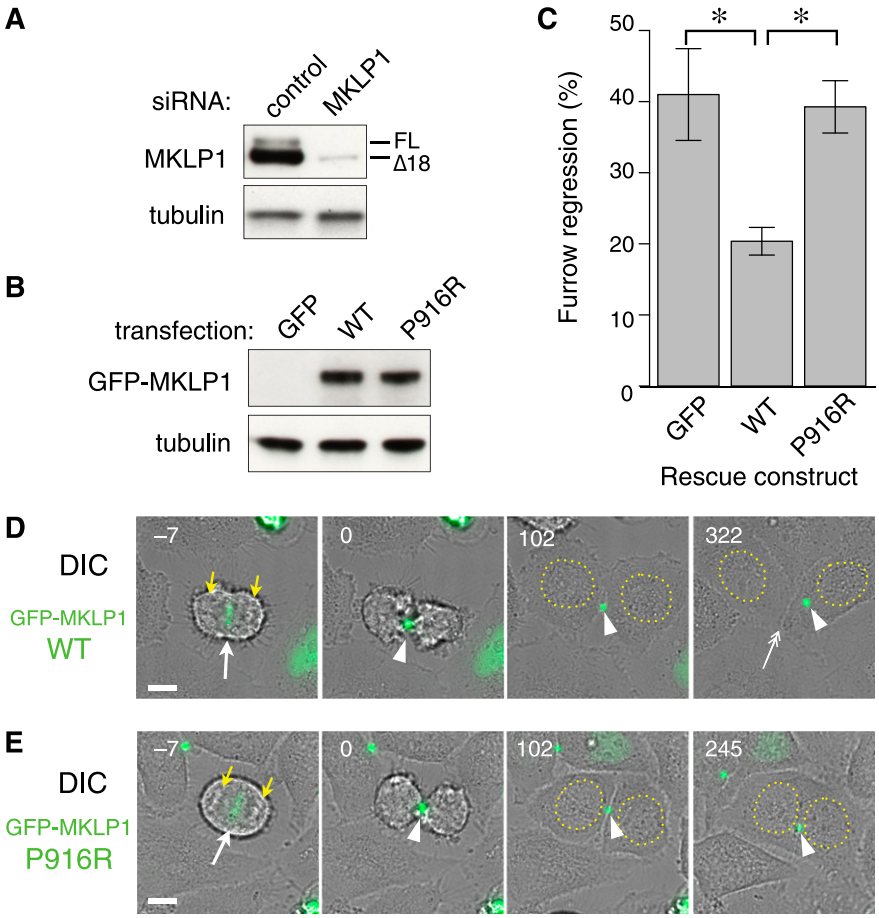

Figure 5. Cytokinesis failure caused by the *KIF23* c.2747C>G (MKLP1 p.P916R) mutation. Efficacy of depletion of endogenous MKLP1 (A) and equal expression of wild-type (WT) and P916R GFP-MKLP1 (B) constructs was confirmed by western blotting of the whole cell lysates with anti-MKLP1 (A) or anti-GFP (B) antibody. Tubulin was also blotted as a loading control. (C) Quantitation of cytokinesis failures from live cell recordings of HeLa cells treated with MKLP1 siRNA and transfected with GFP vector or the MKLP1 variants as indicated. The graph shows the percentage of cells that failed cytokinesis averaged from 3 independent experiments in which at least 80 GFP-MKLP1 or GFP-expressing cells were analyzed (supplemental Table 4). *$P < .001$ after Turkey correction for multiple comparisons. Error bars indicate the standard deviation. (D-E) Stills from the live recordings (A-C) by differential interference contrast (DIC) and GFP fluorescence microscopy. Number indicates the time after midbody formation. GFP-MKLP1 P916R mutant (E) was localized to the spindle midzone (−7 min, arrow) and condensed to form the midbody (0 and 102 min, arrowheads) in a similar manner to the WT GFP-MKLP1 (D). However, the cell membrane of the intercellular bridge was detached from the midbody 217 min after its formation, creating a binucleate cell (245 min). Note that in the WT GFP-MKLP1 cell, abscission happened at 252 min and the 2 daughter cells were separated (D) at 322 min, double arrow. The remnant of the midbody (arrowhead) was incorporated to the cell on the right. Bar, 10 μm. Yellow arrowheads and dotted circles indicate segregating chromosomes and reformed nuclei, respectively.

earlier study, thymidine kinase levels are higher in children and normal ranges for different ages have not been established.[10] In the CDA III–negative group with no available bone marrow smears, none of the patients showed any sign of hemolysis. One 4-year-old child with a thymidine kinase of 30 U/L was considered CDA III–negative because LDH and haptoglobin levels were normal.

For identification of the CDA III causative gene, we used targeted resequencing of the region where the disease was previously mapped. We established a minimal haplotype shared by all affected individuals in the family. This region covered 2.41 Mb and contained 10 genes; however, for practical reasons a 3.54-Mb region with 24 genes was sequenced. To exclude all population-specific normal sequence variants, we compared sequences of a CDA III patient and her unaffected sister. To identify a potential disease mutation, we prioritized sequence variants that are unique for a CDA III–positive patient, are heterozygous, segregate with the phenotype, and are novel or have a frequency <1% in the Single Nucleotide Polymorphism Database. As a result, a novel heterozygous sequence variant in the *KIF23* gene, c.2747C>G (p.P916R), was the most promising candidate as a cause of the disease among 10 CDA III–unique single nucleotide polymorphisms. This mutation was predicted to be damaging for protein function via bioinformatics tools and this point mutation was found only in individuals diagnosed with CDA III and not only in the Swedish family but also in the American family. The Swedish and American CDA III families are, to the best of our knowledge, not related.

KIF23 encodes the kinesin superfamily molecule MKLP1 that plays critical roles in cytokinesis.[19,20] It has a kinesin motor domain on its N terminus and a domain predicted to form a coiled coil in the middle of the molecule. In proliferating cells, it primarily exists as centralspindlin, an evolutionarily conserved stable heterotetrameric complex with CYK4/MgcRacGAP encoded by *RACGAP1*, which binds to the neck region of MKLP1 connecting the motor domain to the coiled coil domain.[21] Both components of centralspindlin are required for proper formation of the central spindle and the midbody. Centralspindlin accumulates to the central antiparallel overlap zone of these microtubule-based structures and recruits various downstream cytokinesis factors to the site of division.[22,23] In our knockdown and rescue experiments, the P916R mutant MKLP1 failed to rescue the cytokinesis failure caused by depletion of the endogenous wild-type molecule, indicating that the p.P916R mutation affects the function of MKLP1 in cytokinesis. This accounts for the characteristic pathological condition of the CDA III (ie, the large multinucleated erythroblasts found in bone marrows of the patients).

Centralspindlin heterotetramers further oligomerize into higher order clusters in vivo enhancing its interaction with microtubules. This plays a crucial role in its sharp accumulation into the midbody,[24] which is important for the stable maintenance of the intercellular bridge through anchorage of the plasma membrane to the midbody microtubule bundles until the final separation of the daughter cells through abscission.[18,25] This unique clustering activity is regulated through the C terminal tail domain of MKLP1. The 14-3-3 proteins, which bind to a short motif containing a phosphorylated serine (S814 in the longest splicing isoform, same hereafter), sequester centralspindlin into an unclustered, inactive state.[17] Phosphorylation of the second serine (S812) within the 14-3-3 binding motif by Aurora B kinase, which is active at the spindle midzone, releases centralspindlin from the sequestration by 14-3-3. ARF6 GTPase, which binds the

MKLP1 C terminal domain in a competitive manner against 14-3-3, colocalizes with centralspindlin on the late midbody and thus prevents premature collapse of the intercellular bridge.[18,26] The p.P916R mutation might affect the stability of the midbody by interfering with these or unknown regulations of centralspindlin clustering. Stable postmitotic maintenance of the midbody is also controlled by phosphorylation of S911 by Aurora B kinase, which prevents collapse of the midbody from premature onset of the nuclear import of centralspindlin driven by a bipartite nuclear localization signal in the tail of MKLP1.[27,28] Thus, interference with this regulation of nuclear import might provide an alternative route to the cytokinesis defect caused by the p.P916R mutation. Future studies with more detailed biochemical and cell biological analyses would be required for testing these possibilities.

The question of why we see multinucleated cells only in the erythropoiesis, but not in other cell lineages in the CDA III patients, remains to be investigated. Although centralspindlin components are essential for cytokinesis in all metazoan cells so far examined, it is becoming clear that it works in the context of a large protein–protein interaction network, which includes other microtubule-bundling proteins whose activities seem to be partially redundant with those of centralspindlin.[29] Indeed, there is a significant difference in expression levels of 1 such microtubule-bundling protein, PRC1, between late epidermal and early neural cells during embryogenesis.[30] We speculate that cells within a living organism might modify the conserved protein–protein network to adapt to the specific requirements from their developmental and physiological conditions. The erythropoiesis-specific cytokinesis failure in CDA III might reflect the lower tolerance of the cells in the erythropoietic lineage to the defect in KIF23/MKLP1 than that of the other cells. Transient cytokinesis failure generates unstable tetraploid cells, which can be transformed into malignant tumors via aneuploidy.[31] Less frequent cytokinesis failure in lymphoid lineage might explain the myeloma and monoclonal gammopathy in CDA III. The mutations in CDAN1 and SEC23B responsible for CDA I and II, respectively, might also be involved in cytokinesis, or more broadly cell division, in the erythropoietic lineage. We believe that deeper knowledge of the molecular mechanism of cytokinesis would contribute to better understanding of these diseases and, ultimately, to improvement of its medical treatments.

Acknowledgments

The authors thank all members of the CDA type III families and acknowledge collaboration with Ambry Genetics, CA. The authors also thank Frida Jonsson for technical assistance in sequencing of candidate genes.

This work was supported by a regional agreement between Umeå University and Västerbotten County Council in cooperation in the fields of Medicine, Odontology, and Health, unrestricted grants from Alexion and Cancerforskningsfonden Norrland, and a program grant from Cancer Research UK (C19769/A11985).

Authorship

Contribution: M.L., A.W., M.M., and I.G. designed the study; M.L., A.W., S.M., and H.S. collected clinical data; A.-L.V. and M.L. performed mutation analyses and expression studies; A.F.I. did functional assays; A.-L.V., A.F.I., A.N., M.M., and I.G. analyzed and interpreted the data; M.L., M.M., and I.G. provided financial support; all authors contributed to the writing process and approved the final manuscript.

Conflict-of-interest disclosure: The authors declare no competing financial interests.

Correspondence: Irina Golovleva, Clinical Genetics, University Hospital of Umeå, 901 85 Umeå, Sweden; e-mail: irina.golovleva@medbio.umu.se; and Masanori Mishima, Mechanochemical Cell Biology, Division of Biomedical Cell Biology, Warwick Medical School, University of Warwick, UK; e-mail: masanori@mechanochemistry.org.

References

1. Heimpel H, Wendt F. Congenital dyserythropoietic anemia with karyorrhexis and multinuclearity of erythroblasts. *Helv Med Acta.* 1968;34(2):103-115.
2. Heimpel H, Wendt F, Klemm D, Schubothe H, Heilmeyer L. Congenital dyserythropoietic anemia [in German]. *Arch Klin Med.* 1968;215(2):174-194.
3. Wickramasinghe SN, Wood WG. Advances in the understanding of the congenital dyserythropoietic anaemias. *Br J Haematol.* 2005;131(4):431-446.
4. Sandström H, Wahlin A, Eriksson M, Bergström I, Wickramasinghe SN. Intravascular haemolysis and increased prevalence of myeloma and monoclonal gammopathy in congenital dyserythropoietic anaemia, type III. *Eur J Haematol.* 1994;52(1):42-46.
5. Wolff JA, Von Hofe FH. Familial erythroid multinuclearity. *Blood.* 1951;6(12):1274-1283.
6. Bergstrom I, Jacobsson L. Hereditary benign erythroreticulosis. *Blood.* 1962;19:296-303.
7. Accame EA, de Tezanos Pinto M. Congenital dyserythropoiesis with erythroblastic polyploidy. Report of a variety found in Argentinian Mesopotamia (author's transl). In Spanish]. *Sangre (Barc).* 1981;26(5-A):545-555.
8. Goudsmit R, Beckers D, De Bruijne JI, et al. Congenital dyserythropoietic anaemia, type 3. *Br J Haematol.* 1972;23(1):97-105.
9. McCluggage WG, Hull D, Mayne E, Bharucha H, Wickramasinghe SN. Malignant lymphoma in congenital dyserythropoietic anaemia type III. *J Clin Pathol.* 1996;49(7):599-602.
10. Sandström H, Wahlin A, Eriksson M, Bergström I. Serum thymidine kinase in congenital dyserythropoietic anaemia type III. *Br J Haematol.* 1994;87(3):653-654.
11. Lind L, Sandström H, Wahlin A, et al. Localization of the gene for congenital dyserythropoietic anemia type III, CDAN3, to chromosome 15q21-q25. *Hum Mol Genet.* 1995;4(1):109-112.
12. Dgany O, Avidan N, Delaunay J, et al. Congenital dyserythropoietic anemia type I is caused by mutations in codanin-1. *Am J Hum Genet.* 2002;71(6):1467-1474.
13. Bianchi P, Fermo E, Vercellati C, et al. Congenital dyserythropoietic anemia type II (CDAII) is caused by mutations in the SEC23B gene. *Hum Mutat.* 2009;30(9):1292-1298.
14. Schwarz K, Iolascon A, Verissimo F, et al. Mutations affecting the secretory COPII coat component SEC23B cause congenital dyserythropoietic anemia type II. *Nat Genet.* 2009;41(8):936-940.
15. Arnaud L, Saison C, Helias V, et al. A dominant mutation in the gene encoding the erythroid transcription factor KLF1 causes a congenital dyserythropoietic anemia. *Am J Hum Genet.* 2010;87(5):721-727.
16. Köhn L, Kadzhaev K, Burstedt MS, Haraldsson S, Hallberg B, Sandgren O, Golovleva I. Mutation in the PYK2-binding domain of PITPNM3 causes autosomal dominant cone dystrophy (CORD5) in two Swedish families. *Eur J Hum Genet.* 2007;15(6):664-671.
17. Douglas ME, Davies T, Joseph N, Mishima M. Aurora B and 14-3-3 coordinately regulate clustering of centralspindlin during cytokinesis. *Curr Biol.* 2010;20(10):927-933.
18. Joseph N, Hutterer A, Poser I, Mishima M. ARF6 GTPase protects the post-mitotic midbody from 14-3-3-mediated disintegration. *EMBO J.* 2012;31(11):2604-2614.
19. Kuriyama R, Gustus C, Terada Y, Uetake Y, Matuliene J. CHO1, a mammalian kinesin-like protein, interacts with F-actin and is involved in the terminal phase of cytokinesis. *J Cell Biol.* 2002;156(5):783-790.
20. Nislow C, Lombillo VA, Kuriyama R, McIntosh JR. A plus-end-directed motor enzyme that moves antiparallel microtubules in vitro localizes to the interzone of mitotic spindles. *Nature.* 1992;359(6395):543-547.
21. Mishima M, Kaitna S, Glotzer M. Central spindle assembly and cytokinesis require a kinesin-like

protein/RhoGAP complex with microtubule bundling activity. *Dev Cell.* 2002;2(1):41-54.

22. Green RA, Paluch E, Oegema K. Cytokinesis in animal cells. *Annu Rev Cell Dev Biol.* 2012;28:29-58.
23. White EA, Glotzer M. Centralspindlin: at the heart of cytokinesis. *Cytoskeleton (Hoboken).* 2012; 69(11):882-892.
24. Hutterer A, Glotzer M, Mishima M. Clustering of centralspindlin is essential for its accumulation to the central spindle and the midbody. *Curr Biol.* 2009;19(23):2043-2049.
25. Lekomtsev S, Su KC, Pye VE, et al. Centralspindlin links the mitotic spindle to the plasma membrane during cytokinesis. *Nature.* 2012;492(7428):276-279.
26. Makyio H, Ohgi M, Takei T, et al. Structural basis for Arf6-MKLP1 complex formation on the Flemming body responsible for cytokinesis. *EMBO J.* 2012;31(11):2590-2603.
27. Neef R, Klein UR, Kopajtich R, Barr FA. Cooperation between mitotic kinesins controls the late stages of cytokinesis. *Curr Biol.* 2006;16(3):301-307.
28. Liu X, Erikson RL. The nuclear localization signal of mitotic kinesin-like protein Mklp-1: effect on Mklp-1 function during cytokinesis. *Biochem Biophys Res Commun.* 2007;353(4):960-964.
29. Lee KY, Davies T, Mishima M. Cytokinesis microtubule organisers at a glance. *J Cell Sci.* 2012;125(Pt 15):3495-3500.
30. Kieserman EK, Glotzer M, Wallingford JB. Developmental regulation of central spindle assembly and cytokinesis during vertebrate embryogenesis. *Curr Biol.* 2008; 18(2):116-123.
31. Fujiwara T, Bandi M, Nitta M, Ivanova EV, Bronson RT, Pellman D. Cytokinesis failure generating tetraploids promotes tumorigenesis in p53-null cells. *Nature.* 2005;437(7061): 1043-1047.